HYDRODYNAMIC CONDITIONS IN A FIXED THREE-PHASE GRANULAR LAYER. EXPERIMENTAL INVESTIGATION

B. L. Ogarkov, V. A. Kirillov, and V. A. Kuzin

UDC 532.546

An experimental investigation of the hydrodynamic conditions in a three-phase granular layer for direct upward flow of a gas and a liquid has been performed. The floating-up speeds of gas bubbles and pistons have been determined for different operating conditions. A diagram of hydrodynamic conditions has been plotted.

A theoretical analysis of direct upward flow of a gas–liquid mixture through a fixed granular layer was performed in [1], and a number of stipulations concerning the determination of the hydrodynamic conditions have been proposed. Our aim was to check experimentally the proposed inequalities and determine the parameters of the hydrodynamic models necessary for plotting a chart of the operating conditions. There are several known papers on the investigation of hydrodynamic conditions in vertical and horizontal pipes pertaining to two-phase flow [2, 3].

Hydrodynamic conditions were classified in [2] with respect to pressure pulsations at the pipe wall, measured by means of tensometric data units. An electrochemical method was used for this purpose in [3], and the flow conditions were determined with respect to the diffusion current. In all these papers, the motion of the bubbles was considered as a steady-state random process, and the sets of conditions were classified with respect to the type of spectral density. There is a paper [4], perhaps the only one, concerned with granular layers, where the hydrodynamic conditions are investigated by means of electric-contact data units.

Experimental Method and Device

We have investigated the hydrodynamic conditions by means of the capacitance method. This method is virtually inertialess; it is characterized by a high resolving power, and it permits work with any medium and the use of insulated electrode surfaces. This is an important advantage in comparison with other methods. Our method is based on measuring the permeability of the medium at the surface of the data unit. The permeability is related directly to the local gas percentage and the hydrodynamic conditions of the gas–liquid flow in the free volume of the layer. The block diagram of the experimental device is shown in Fig. 1. Gas (air) and water are supplied through a system of rotameters to column 1 by direct upward flow. The column is filled with packing consisting of glass balls. A spherical capacitive data unit is placed inside the layer. The data unit consists of a hollow sphere, where cylinders (first electrode) with needles (second electrode) positioned coaxially inside the cylinders are mounted at five points of the sphere The sensing elements are mounted flush with the sphere surface. The diameters of the data units match those of the packing balls; they are equal to 18 and 8 mm. Only one set of electrodes is mounted in the 8-mm data unit. The data unit is connected to one arm of the compensating bridge 3, which is supplied from an audiofrequency oscillator with ac current at a frequency of 200 kHz. The bridge unbalance caused by the passage of bubbles is supplied in the form of an analog signal to the input of an IRA-5 computer (4, Fig. 1), where primary processing of the information is performed by means of program I: interrogation of the data units, zero line shift, and formation of banks. After the necessary amount of discrete information has been

Institute of Catalysis, Siberian Branch, Academy of Sciences of the USSR, Novosibirsk. Translated from Inzhenerno-Fizicheskii Zhurnal, Vol. 31, No. 5, pp. 800-806, November, 1976. Original article submitted April 14, 1975.

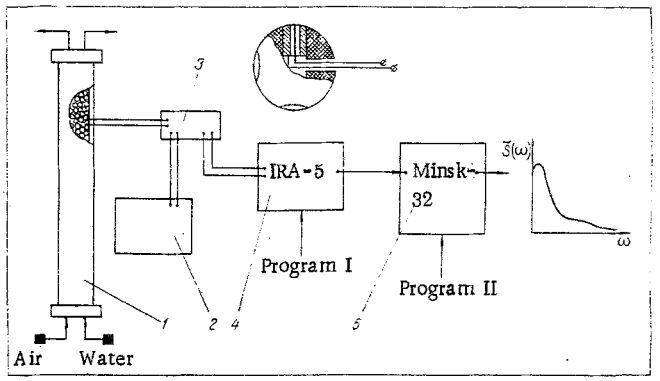

Fig. 1. Block diagram of the experimental device: 1) column; 2) audiofrequency oscillator; 3) compensating bridge; 4) IRA-5; 5) Minsk-32. (The cross-section of the data unit is shown at the top.)

received and processed, the IRA-5 computer transmits the signals in digital code through a communication channel to a Minsk-32 computer (5). The latter performs complete processing, including calculation of the mathematical expectation, the autocorrelation function, and the spectral density, and provides at the ADP the necessary number of diagrams.

It should be mentioned that the use of a hierarchical computer system is very efficient in experimental investigations, since the duration of a single experiment, including processing, does not exceed 3-4 min.

The experimental conditions were as follows: column diameter, D = 100 mm; column height, 2 m; packing, 18- and 8-mm balls. The gas velocity, calculated for the total cross section, was equal to 5-300 m/sec, while the liquid velocity was equal to 1.0-15 cm/sec.

In order to determine the quantitative relationships, the data units were calibrated together with the computer under static conditions. In this, the relationship between the film thickness at the grain surface and the readings of the IRA-5 computer was determined. It was found that this relationship is nonlinear and that the maximum film thickness that can be determined reliably lies within the range 0-1.5 mm.

The experimental investigations were performed for wetted and nonwetted data-unit surfaces. In the latter case, the surfaces of the packing balls and the data unit itself were coated with silicone varnish and were then put into the column.

In order to ensure a sufficiently high statistical reliability of the results of measurements based on the method described in [5, 6], we used the following conditions: recording time, 40 sec; number of recording points, 2000; discreteness interval, 0.02 sec.

The estimate of the autocorrelation function was obtained by means of the computer on the basis of the expression

$$R(\tau) \approx R(m) = \frac{1}{N-m+1} \sum_{n=1}^{N-m} X(n)\, X(n+m). \tag{1}$$

The smoothing-out was then performed by using the spectral window proposed by Hann [5]:

$$D(\tau) = \frac{1}{2}\left(1 + \cos\frac{\tau}{\tau_m}\right). \tag{2}$$

After this, the normalized estimate of the spectral density was determined:

$$\tilde{S}(\omega) = \frac{\frac{2}{\pi}\sum_{i=1}^{N} R(\tau)\exp(i\omega\tau)}{\sum_{i=1}^{N} S(\omega)}. \tag{3}$$

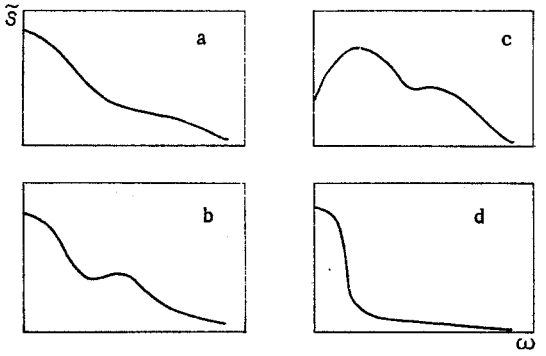

Fig. 2. Characteristic types of spectral density. a) Bubble conditions; b) shell conditions; c) piston conditions; d) annular-dispersion conditions.

Figure 2 shows the most characteristic types of spectral density for different sets of hydrodynamic conditions. As in [2, 3], these dependences characterize bubble (a), shell (b), piston (c), and annular-dispersion (d) conditions.

Besides investigating the hydrodynamic conditions, we also performed experiments on determining the speed with which bubbles, shells, and pistons float up through the granular layer. In this case, two electric-contact data units made of surgical needles with different diameters were used instead of the capacitative data unit. The experimental method consisted in determining the time in which a bubble passes through a section of a certain length. Preliminary experiments with standard-size bubbles in a bubbling column have shown that this time can be determined with respect to the distance between the maxima of the cross-correlation function calculated by means of the expression

$$R_{xy}(\tau) \approx R(m) = \frac{1}{N-m+1} \sum_{n=1}^{N-m} X(n)\, Y(n+m). \tag{4}$$

Determination of the Parameters of Hydrodynamic Models

a) Thickness of the Liquid Film on the Side Surface of Grains. In the physical sense, the thickness δ coincides with the mathematical expectation of a random process, and it corresponds to the statistical mean of the distance between the passing bubbles and the grain surface. Experimental investigations have shown that the film thickness depends strongly on the grain position in the layer. Thus, the value of δ is at a maximum in the neighborhood of the contact points of particles and is at a minimum in regions of intensive bubble motion. The mean thickness values were determined by summing the readings from all five data units, located at different points of the grain. The results obtained are given in Fig. 3a. This figure also shows the local gas percentages at the grain surface, which were obtained by dividing the film thickness by the sensitivity zone of the data unit, i.e.,

$$\varphi = 1 - \frac{\delta}{1.50}. \tag{5}$$

Figure 3b shows the statistical mean of the part of the side surface of the grain occupied by the gaseous phase as a function of the local gas percentage and the wettability conditions per realization interval. An analysis of these results indicates that virtually the entire grain is covered with a liquid film for $\varphi < 0.3$. This agrees with the conclusion reached earlier in [4]. The effect of wettability (or the surface-tension coefficient) manifests itself only at high gas percentages.

b) Floating-up Velocity of Gas Bubbles. According to [1], in steady-state motion through a granular layer, the bubble velocity is determined from the balance of the forces of drag, deformation, and lift, i.e.,

$$u = \frac{1}{9} \cdot \frac{gR_0^2}{\nu} \cdot \frac{(1-\varepsilon)^2}{(1-\varepsilon^{5/3})} \left(1 - \frac{3}{2}\, \text{Eö}\, C\right). \tag{6}$$

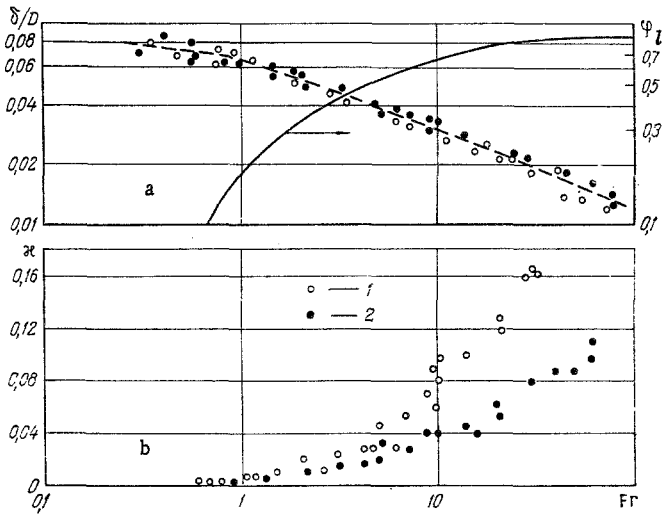

Fig. 3. Statistical mean values of the physical parameters. a) Mean thickness of the liquid film and local gas percentage; b) part of the grain surface occupied by the gaseous phase per realization interval; 1) wetted surface; 2) nonwetted surface (coated with silicone varnish).

The value of C reflects the effect of the geometric structure of the layer on the floating-up speed and can be determined experimentally. Thus, analysis of data on the floating-up velocity for 18- and 8-mm packings shows that $C \approx 0.64$; the bubble radius was calculated on the basis of the Taylor instability,

$$R_0 \approx \sqrt{\frac{\sigma}{g(\rho_2 - \rho_1)}}. \tag{7}$$

It should be noted that, for a packing consisting of 18-mm balls, the value of R_0 calculated on the basis of (7) is close to the hydraulic radius [7],

$$R_0 = \frac{2}{3}\,\frac{\varepsilon}{1-\varepsilon} R - \delta. \tag{8}$$

c) The Velocity of Slowed-Down Bubbles. The velocity of slowed-down bubbles was determined for a spacing between the electrodes equal to the radius of a packing element. Balls with d = 18 mm were used in this case. The experimental results were processed by using the theoretical relationships given in [1]. The processing consisted in the following: the time of passage through the control section was determined with respect to the interelectrode spacing, and this time was used to determine the integral mean velocity during the period the bubbles were moving closer to one another. Comparison between theoretical calculations and experimental data made it possible to determine the angle α [1] as a function of the gas velocity. Thus, $\alpha \approx 0.21$ for $u_1 = 2$ cm/sec, while $\alpha = 0.16$ for $u_1 = 2$ cm/sec.

d) Velocity of Liquid (Gas) Pistons. Under conditions of steady motion, the piston velocity can be determined from the balance of drag and gravitational forces, i.e.,

$$\rho_2 g = \Delta p. \tag{9}$$

Since $\Delta p = \xi[\rho_2 (u_3^0)^2/2] \cdot S_{sp}/\varepsilon$, while the drag coefficient can be found from $\xi = A/Re + B$ by analogy with single-phase flow through a granular layer, then

$$u_3^0 = \frac{A\nu}{Bd}\left(-1 + \sqrt{1 + \frac{2g\varepsilon Bd}{S_{sp}A^2\nu^2}}\right). \tag{10}$$

Expression (10) determines the velocity of a piston under "free" conditions. If the distance between pistons is small (if it is of the order of the column radius), then, as in the case of the upward movement of air shells, the velocities can be somewhat higher than is indicated by (10) because of the interaction between shells.

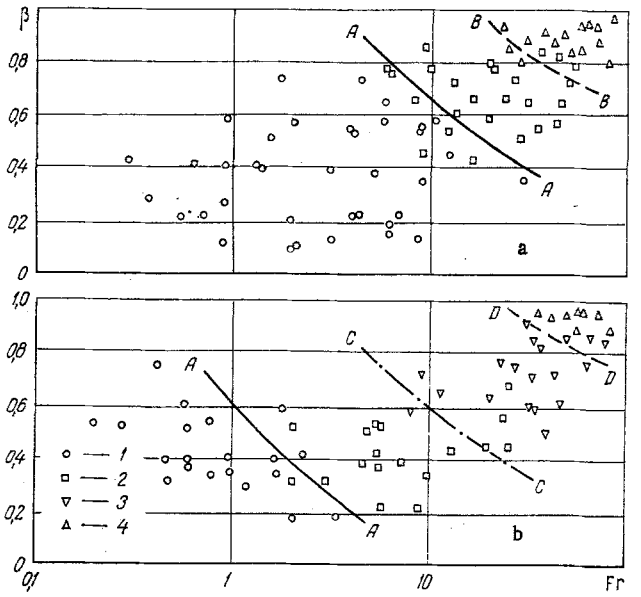

Fig. 4. Diagrams of hydrodynamic conditions in a fixed three-phase granular layer. a) Ball packing, d = 18 mm; b) ball packing, d = 8 mm; 1) bubbles; 2) upward motion of shells; 3) upward motion of pistons; 4) annular-dispersion conditions; A–A, B–B, C–C, and D–D) theoretical boundaries between different sets of conditions.

In this case, by analogy with [8],

$$u_3 = u_3^0 \left[0.35 + 2.8 \exp\left(-\ 1.06\ \frac{L}{D}\right)\right]. \qquad (11)$$

The change in the relative distance between pistons, depending on the gas and liquid velocities, can be calculated with an accuracy to ±15% by using the following relationships: $L/D = 1.25\ Fr^{-0.06}$ for $Fr < 0.4$ and $L/D = 1.1\ Fr^{-0.20}$ for $Fr > 0.4$. The calculations were performed for the values A = 75.0 and B = 0.875, which correspond to single-phase flow through a granular layer [7].

Diagram of Hydrodynamic Conditions in the Packing Layer

The diagram was plotted on the basis of the theoretical relationships obtained earlier in [1] for calculating the conditions for the switch of operating conditions and the experimental results obtained in our work. The experimental method for determining the existence conditions and the transition boundaries was described earlier. The results obtained are given in Fig. 4a for a layer consisting of balls with d = 18 mm and Fig. 4b for d = 8 mm. The solid curves in the figure correspond to the theoretical transition boundaries. As follows from Fig. 4a, b, the relationships obtained in [1] on the whole accurately reflect the hydrodynamic conditions in a fixed layer and can be used for practical applications. The slight scatter of the experimental data is evidently due to the presence of uncontrollable parameters, for instance, the purity of water. The latter exerts a considerable effect on the surface-tension coefficient.

NOTATION

$R(\tau)$	is the autocorrelation function;
n, m	are the discrete arguments of the correlation function;
τ	is the displacement time;
N	is the number of discrete realization ordinates;
τ_m	is the maximum shift;
ω	is the frequency;
$S(\omega)$	is the spectral density;
δ	is the thickness of the liquid film;

u is the bubble velocity;
R_0 is the bubble radius;
ε is the porosity;
ν is the kinematic viscosity;
σ is the surface-tension coefficient;
g is the acceleration due to gravity;
R is the radius of packing grain, $d = 2R$;
u_3 is the piston velocity;
Fr, Eö are the Froude and Eötvös numbers, respectively;
ρ_2, ρ_1 are the densities of liquid and gas, respectively;
L is the distance between pistons;
D is the column diameter;
S_{sp} is the specific surface of the packing;
φ_l is the local gas percentage at the side surface of grains;
β is the volumetric gas percentage.

LITERATURE CITED

1. V. A. Kirillov, B. L. Ogarkov, and V. G. Voronov, Inzh.-Fiz. Zh., 31, No. 3 (1976).
2. Advances in the Field of Heat Exchange [Russian translation], Mir, Moscow (1970), p. 7.
3. Investigation of the Turbulent Flow of Two-Phase Media [in Russian], Nauka, Novosibirsk (1970).
4. M. A. Kasamanyan, Author's Abstract of Candidate's Dissertation, Novosibirsk (1974).
5. J. S. Bendat and A. G. Piersol, Random Data: Analysis and Measurement Procedures, Wiley (1971).
6. E. G. Dudnikov et al., Mathematical Simulators of Chemical Technology Systems [in Russian], Khimiya, Leningrad (1970).
7. M. É. Aérov and O. M. Todes, Hydraulic and Thermal Principles of the Operation of Apparatus with Fixed Granular Layers and Fluidized Beds [in Russian], Khimiya, Leningrad (1968).
8. Moisis and Griffis, Teploperedacha, Ser. C, 84, No. 1 (1962).

EFFECTIVE DENSITY OF A FLUIDIZED BED

Yu. I. Zinov'ev

UDC (631.358.45+66.096.5):001.5

Pressure coefficients have been determined for a fluidizing agent flowing around a sphere. A method is presented for calculating the integral aerodynamic force; formulas are given for the variation in the apparent aerodynamic density and effective density for a fluidized bed.

If a fluidized bed is to be used as a means of separating materials by density, one needs to know the effective density corresponding to the actual upthrust on an immersed body. Not much is known about the exact origin of this force or the factors that affect it. The effects of a fluidized bed on an immersed sphere have been equated to those of an Archimedean liquid. The density of the pseudofluid has been taken as that of the mass of the grains of solid per unit volume of the suspension. The observed forces differ from the Archimedean value in both senses, which is due to the pressure exerted by the body of grains in the stagnant zone [1, 2, 12] and also to rising currents of the solid [3] or of the solid and fluidizing agent together [14]. It has also been claimed [8, 14] that the force increases with the fluidization number and as the size of the body decreases.

The structure of a fluidized bed near an immersed body differs substantially from that in an unperturbed part of the bed: the aerodynamic wake above the body has a stagnant zone with little circulation in the grains

All-Union Scientific-Research Institute of Agricultural Mechanization, Moscow.

Translated from Inzhenerno-Fizicheskii Zhurnal, Vol. 31, No. 5, pp. 807-814, November, 1976. Original article submitted November 14, 1975.